



\*\*\*\*\*This Document is Under Minor Revision and Formatting \*\*\*\*\*

Tiako P.F. (ed) *Competitive Tools, Techniques, and Methods*. Chronicle of Computing. OkIP. CEST24#17

© 2024 Oklahoma International Publishing

[https://doi.org/10.55432/978-1-6692-0007-9\\_9](https://doi.org/10.55432/978-1-6692-0007-9_9)

# Strategic Energy Management System for Improving the Power Quality of PV-Wind-Battery-based Standalone Microgrids

Wulfran Fendzi Mbasso<sup>1\*</sup>, fendzi.wulfran@yahoo.fr  
Reagan Jean Jacques Molu<sup>1</sup>, molureagan@yahoo.fr  
Serge Raoul Dzone Naoussi<sup>1</sup>, sdzone@gmail.com  
Harrison Ambe<sup>2</sup>, ambe.harrison@ubuea.cm  
Emmanuel Fendzi Donfack<sup>3,4,5</sup>, fendziemmanuel@yahoo.fr  
Kenfack Tsobze Saatong<sup>1,6</sup>, saakenft@yahoo.fr

<sup>1</sup>Technology and Applied Sciences Laboratory, U.I.T. of Douala, P.O. Box 8689 – Douala, University of Douala, Cameroon.

<sup>2</sup>Department of Electrical and Electronics Engineering, College of Technology (COT), University of Buea, P.O. Box Buea 63.

<sup>3</sup>Nonlinear Physics and Complex Systems Group, Department of Physics, The Higher Teacher's Training College, University of Yaoundé I, P.O. Box47, Yaounde, Cameroon.

<sup>4</sup>Pure Physics Laboratory, Group of Nonlinear Physics and Complex Systems, Department of Physics, Faculty of Sciences, University of Douala, P.O. Box24157, Douala, Cameroon.

<sup>5</sup>Laboratory of Mechanics, Materials and Structures, Department of Physics, Faculty of Science, University of Yaoundé I, P.O. Box 812, Yaoundé, Cameroon.

<sup>6</sup>Unité de Recherche d'Automatique et d'Informatique Appliquée, I.U.T. Fotso Victor, P.O. Box 134 – Bandjoun, University of Dschang, Cameroon.

(\*) Corresponding author: Wulfran Fendzi Mbasso; E-mail: fendzi.wulfran@yahoo.fr

**Abstract:** The global community is currently engaged in the exploration of various techniques to utilize renewable energy sources with the objective of mitigating the effects of global warming and decreasing dependence on fossil fuels. The deployment of solar and wind energy has experienced substantial adoption in various geographical areas worldwide. However, the predictability and controllability of solar irradiance and wind speed are constrained. Therefore, it is crucial to incorporate an energy storage system to optimize the utilization of these energy sources by converting them into electrical energy. Within the domain of medium power applications, batteries are recognized as a prominent selection. However, batteries require significant maintenance and are susceptible to self-discharge, resulting in a gradual decrease in storage capacity over time. Hydrogen storage is a feasible alternative for high-power applications, offering a cost-efficient solution in comparison to batteries. The stored hydrogen can be utilized for various applications, including transportation and electricity generation. An electrolyzer is an electrochemical device that employs electrical energy to efficiently perform the process of water electrolysis, which involves the decomposition of water into its elemental components, namely oxygen and hydrogen. Nevertheless, the slow heat transfer dynamics hinder the rapid generation of hydrogen, necessitating the implementation of a novel control technique to improve production efficiency in response to changes in solar irradiance and wind speed. The deployment of boost, buck, and DC to DC bidirectional converters is utilized to maintain a consistent voltage at the DC-link across different operational scenarios. A novel control algorithm has been developed to ensure power quality at the 3-phase AC load bus and efficiently manage energy in the hybrid standalone system. The outcomes of this inquiry, conducted utilizing MATLAB/Simulink, are exhibited to evaluate the efficiency in various scenarios.

**Keywords:** Renewable Energy, Solar and Wind Energy, Energy Storage System, Batteries, Hydrogen Storage, Control Algorithm.

## I. Introduction

Delivering electrical power to consumers in areas lacking utility grids continues to present a complex undertaking. To mitigate this problem, the adoption of small-scale autonomous microgrids at a local level can be regarded as a more feasible alternative. The microgrids employ renewable energy sources, making them ecologically sustainable [1-4]. Through the integration of diverse renewable energy sources, such as solar power utilizing Photovoltaic (PV) technology and wind power utilizing Permanent Magnet Synchronous Generator (PMSG) technology [1], these systems have the capability to deliver dependable and high-standard electricity to consumers situated in remote areas.

The solar irradiance and wind velocity experience continuous variations, resulting in fluctuations in power generation. To maintain a stable power balance within a self-contained microgrid, it is crucial to utilize an energy storage device. While

batteries are commonly used for energy storage, they may not be optimal for extended high-power applications. In addition, batteries have a limited lifespan and necessitate regular maintenance and replacements, resulting in increased expenses. In order to tackle these challenges, the system incorporates a Fuel Cell (FC)-Electrolyzer alongside a compact battery storage system. The battery bank demonstrates high responsiveness to sudden changes, while the FC-Electrolyzer operates at a slower pace to maintain power equilibrium in a stable condition. During periods of surplus power generation compared to the demand, the FC-Electrolyzer employs the process of electrolysis to generate hydrogen. This hydrogen is then stored in tanks for future use in generating electricity through a fuel cell (FC) system, in order to meet the load requirements. By employing a battery bank as a means of providing power for a limited duration and utilizing hydrogen as a method of storing energy for extended periods, the system achieves enhanced economic feasibility. However, the deployment of efficient energy management is crucial to ensure optimal power quality in standalone systems. Moreover, this document showcases the deployment of an inverter control mechanism designed to maintain a consistent voltage at the load bus, even when faced with unbalanced voltage conditions. This mechanism is designed to enhance power quality.

## II. Standalone Microgrid

The schematic in Figure 1 illustrates the autonomous microgrid that is dependent on renewable energy sources, as described in this document.

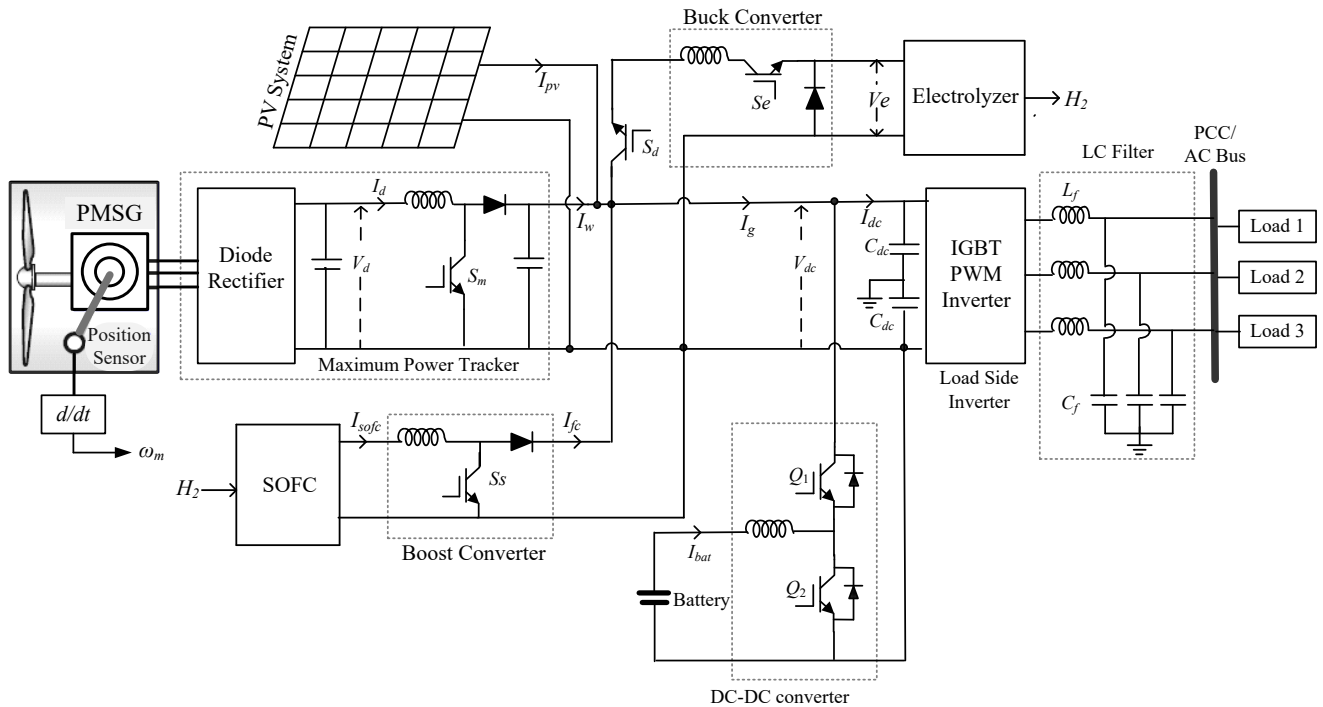


Figure 1: Hybrid standalone microgrid.

A multitude of researchers have conducted empirical investigations on the hybrid microgrid with comparable standalone characteristics in prior scholarly articles [7-13]. An author proposed a power management strategy to regulate the various components within the microgrid [7]. The authors in [8] presented a study showcasing the production of hydrogen using power conversion units that are dependent on renewable energy sources. However, as mentioned in reference [9], a greenhouse was established that is powered by renewable energy sources. However, it is important to acknowledge that the system was specifically designed and optimized for single-phase applications. The researchers outlined the methodology for hydrogen production using renewable energy sources, as documented in reference [10]. Nevertheless, the analysis conducted did not include any discussion or examination of power quality. The authors in [11] proposed the implementation of a direct current (DC) microgrid that utilizes renewable energy sources for the production of hydrogen. Moreover, research conducted in [12] introduced an energy management algorithm specifically tailored for a microgrid. Nevertheless, it did not consider power quality concerns and situations with imbalanced conditions. Finally, a study was conducted to perform a comparative evaluation of different energy management systems for standalone wind, photovoltaic (PV), wind, and hydrogen units [13]. This research article addresses the aforementioned objectives in its development.

- A highly effective control coordination mechanism has been successfully implemented to oversee the operations of wind, photovoltaic (PV), electrolyzer, fuel cell (FC), and battery systems.
- A novel control technique has been developed for a bidirectional direct current (DC) to direct current (DC) circuit that is utilized between the battery and DC-link to effectively regulate the power distribution among all devices.
- A robust control system has been deployed to effectively manage the voltage at the load bus in response to fluctuations in wind or photovoltaic (PV) power generation and variations in the load.
- Ensuring balanced voltages is essential for maintaining stable voltage levels at the load bus in the presence of unbalanced currents in a three-phase system.

The DC-link battery bank features an integrated DC to DC bidirectional circuit. The control methodology of the circuit is utilized to monitor the discharging/charging process of the battery in order to maintain a constant voltage at the DC link, as illustrated in Figure 2. The output of the controller serves as the reference signal for the battery line current. A hysteresis loop is established in order to generate the necessary switching pulses for the switches Q1 and Q2 of the converter (refer to Figure 1). In order to regulate the charging and discharging of the battery bank, the controller of the DC-to-DC bidirectional circuit includes the State of Charge (SoC) feature, as depicted in Figure 2.

Once the battery bank reaches its maximum level, the state of charge (SoC) will enable the surplus power to be directed towards the electrolyzer in order to produce hydrogen. During a state of steady equilibrium, when the State of Charge (SoC) reaches its minimum threshold, the fuel cell (FC) will generate the requisite power to meet the load demand. However, due to slow response times, the frequency converter (FC) is incapable of instantaneously supplying power, resulting in a decrease in voltage at the direct current (DC) link during transient situations. To ensure a constant voltage at the DC-link, regardless of system variations, it is crucial to establish efficient control coordination among all components in a standalone system. Figure 3 and Figure 4 depict the appropriate control mechanisms for the buck circuit (employed for the electrolyzer) and the boost circuit (employed for the fuel cell), respectively. The controllers designed for the buck, boost, and DC to DC converters are configured in a manner that allows the battery bank to demonstrate instantaneous response to sudden changes in load, while maintaining consistent operation for the electrolyzer-fuel cell (FC) system. When the State of Charge (SoC) reaches 20.0% and switch Q<sub>2</sub> of the DC-DC circuit is activated (while Q<sub>1</sub> is deactivated), the Fuel Cell (FC) stacks initiate the generation of the necessary load power, while the battery maintains its state  $V_{dc}^*$  across the dc-link. Figure 5 illustrates the graphical representation of the energy management system. To optimize the power extraction from a wind turbine, the control strategy is derived from the reference [1]. In order to eliminate the need for an additional converter that functions as a maximum power point tracking (MPPT) circuit, the photovoltaic (PV) system is directly connected to the DC-bus. The Photovoltaic (PV) system utilizes a Maximum Power Point Tracking (MPPT) mechanism that is combined with a DC-to-DC circuit and a buck circuit for the electrolyzer. This integrated setup functions as the MPPT circuit for the PV system. Within a distribution power system, there are multiple single-phase loads that are operating simultaneously, leading to uneven currents flowing through the three phases. When encountering imbalanced loads, the DC-link voltage will display a second harmonic oscillating component. The existence of the second harmonic component has the ability to induce oscillations on the turbine shaft, which can potentially impact the fatigue strength of the shaft. To mitigate the impact of the second harmonic, the controllers of the battery's DC-to-DC converter, the electrolyzer's buck converter, and the fuel cell's boost converter are equipped with a dc-side active filter [14]. The direct current (DC) component ( $V_{dc}'$ ) is extracted through a low pass filter from  $V_{dc}$  and the oscillating component ( $V_{dco}$ ) is obtained from  $V_{dc}'$  and  $V_{dc}$ . The first PI controller takes the error ( $V_{dc}^* - V_{dc}'$ ) into account to generate a reference signal for voltage regulation, while the second PI controller utilizes the error ( $0 - V_{dco}$ ) as its input. The second proportional-integral (PI) controller employs a reference signal of '0' to efficiently eliminate the oscillating component in the direct current (DC) voltage. Through the summation of the outputs of two proportional-integral (PI) controllers, the desired reference current is achieved.

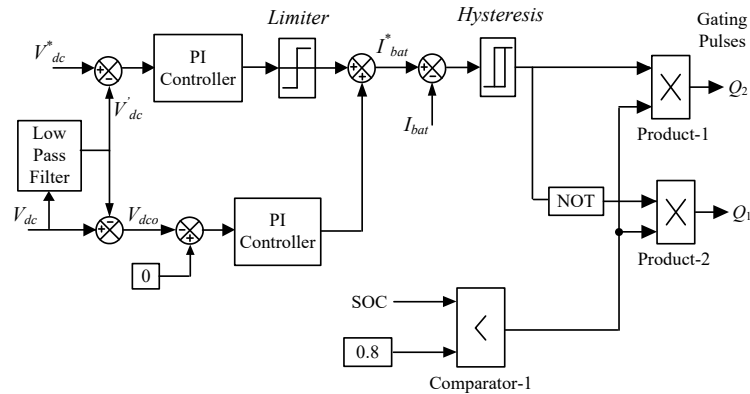


Figure 2: The management of the bidirectional DC to DC circuit linked to the battery is under control.

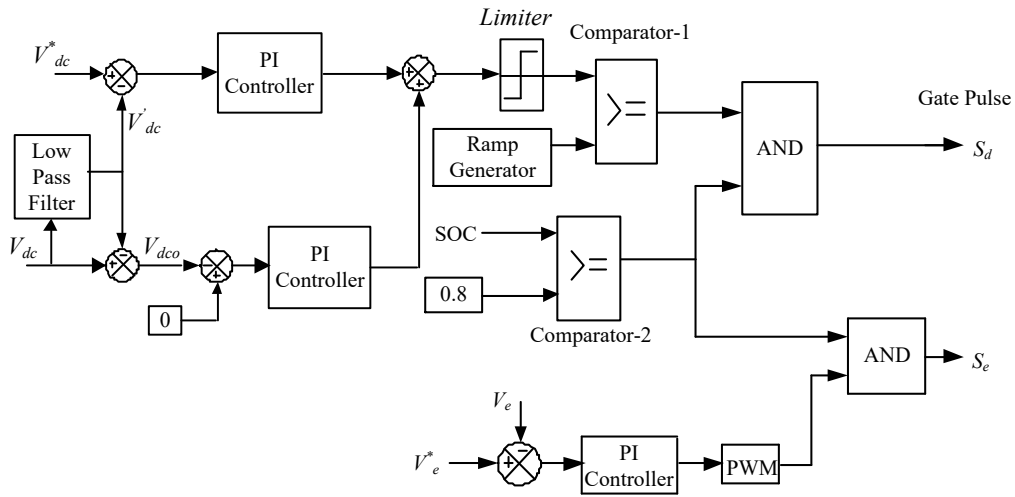


Figure 3: Control of buck converter for electrolyzer.

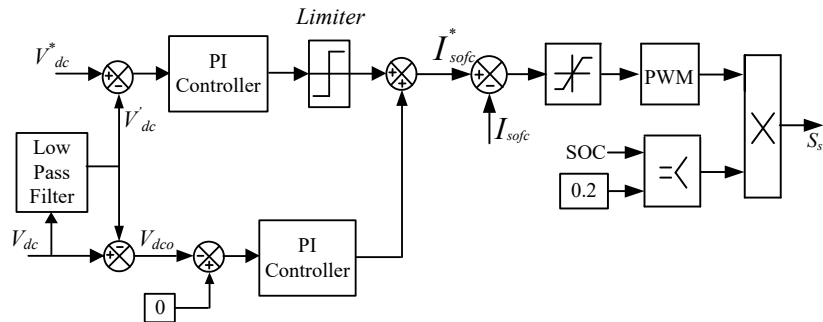


Figure 4: Control of boost converter for FC.

An unbalanced voltage condition arises when there is an uneven distribution of load among the three phases at the point of common coupling (PCC). The observed asymmetry is a result of the non-uniform distribution of voltage drops across the filter circuit in each phase. To address this problem, a dedicated inverter controller has been developed. The controller employs a proprietary algorithm to compute modulation indexes for every phase, leading to the production of well-balanced voltages at the Point of Common Coupling (PCC). The implementation of the control algorithm, which is based on the dq0 transformation of the inverter, is depicted in Figure 6.

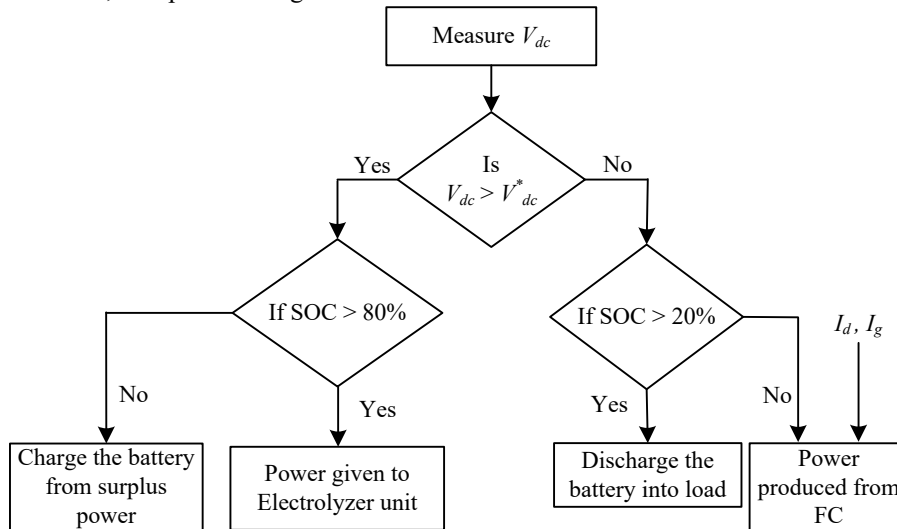


Figure 5: Energy management algorithm.

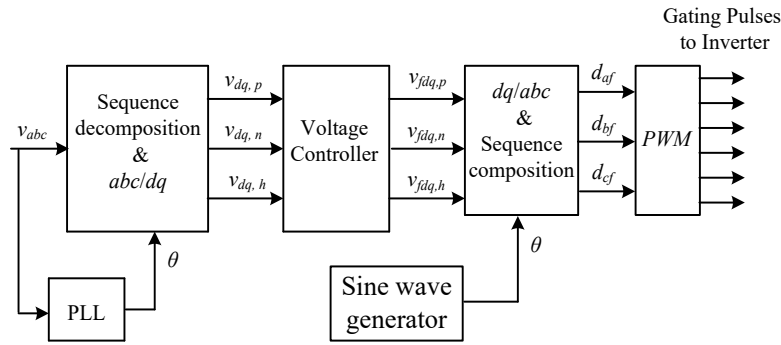


Figure 6: Proposed control of the inverter.

### III. Unit management

Evaluating the optimal unit size is a crucial factor in a microgrid, particularly in scenarios where it relies on renewable energy sources. This is of utmost importance as it contributes to the reduction of the system's overall cost while guaranteeing a dependable and consistent power supply to consumers [15-16]. To accomplish this, the HOMER software is utilized for the computation of the optimal dimensions of the components, taking into consideration the load profile [7], as depicted in Figure 7. The technical and economic data of the system is obtained from the references [7, 15, 17]. By employing the HOMER software, a comprehensive analysis has been performed to ascertain the most suitable dimensions of the wind and PV components. The findings suggest that the wind component should be sized at 15.0kW, while the PV component should be sized at 20.4kW. Consequently, this study investigates the installation of two photovoltaic (PV) arrays, each with a capacity of 7.50 kilowatts (kW), and three wind turbines, each with a capacity of 6.80 kW.

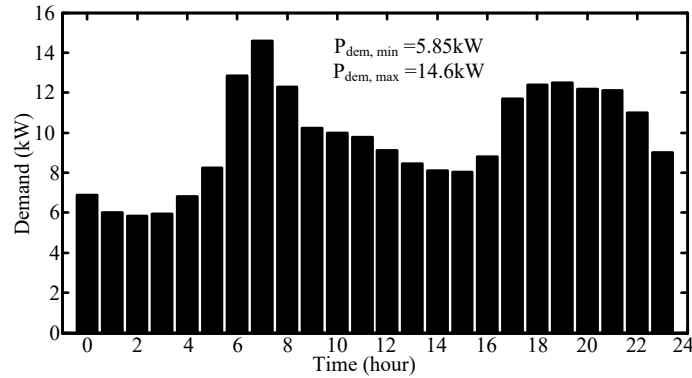


Figure 7: Load demand [7].

In this research, it is anticipated that the fuel cell (FC) will effectively handle the peak load without being dependent on wind and photovoltaic (PV) power. Therefore, the necessary capacity of the fuel cell (FC) is determined to be 18 kilowatts (kW), with an extra 20% capacity allocated for optimal performance. Similarly, the rating of the electrolyzer is determined by evaluating the amount of excess power that is currently available. By considering 60.0% of the maximum surplus power derived from various sources, the rating of the electrolyzer is determined using the following calculation:

$$\begin{aligned} \text{Electrolyzer Rating} &= (\text{Total generation} - \text{Minimum load demand}) \times 60.0/100. \\ &= (15.0+20.40-5.85) \times 0.60=17.73\text{kW}. \end{aligned}$$

### IV. Results

To enhance visualization efficiency, the MATLAB/Simulink platform displays the outcomes by utilizing a solitary photovoltaic (PV) array and a solitary wind turbine. The evaluation of controller performance involves analyzing different scenarios of the microgrid illustrated in Figure 1.

#### Case-A: Unbalanced operation

The system has been tested taking into account the unbalanced scenario illustrated in Figure 8.

Current (RMS) of: Phase-A ( $i_{la}$ )= 3.52A; Phase-B ( $i_{lb}$ )= 9.45A; Phase-C ( $i_{lc}$ )= 8.32A.

Figure 9 depicts the torque response of the Permanent Magnet Synchronous Generator (PMSG) when it is in an imbalanced state. The figure shows the torque response both with and without the recommended control of the DC-to-DC converter. The aforementioned controller, when utilized in tandem with voltage regulation at the DC-link, possesses the capacity to mitigate torque fluctuations. Nevertheless, due to the uneven drops occurring at the LC filter in each phase, there will be an imbalance in the voltages at the Point of Common Coupling (PCC). The proposed inverter controller ensures balanced voltages by generating the necessary modulation indexes for each phase. Figure 10 illustrates the balanced line

voltages measured at the Point of Common Coupling (PCC). In order to improve comprehension, Figure 11 presents the root mean square (RMS) values of the phase voltages and their corresponding modulation indexes (MI).

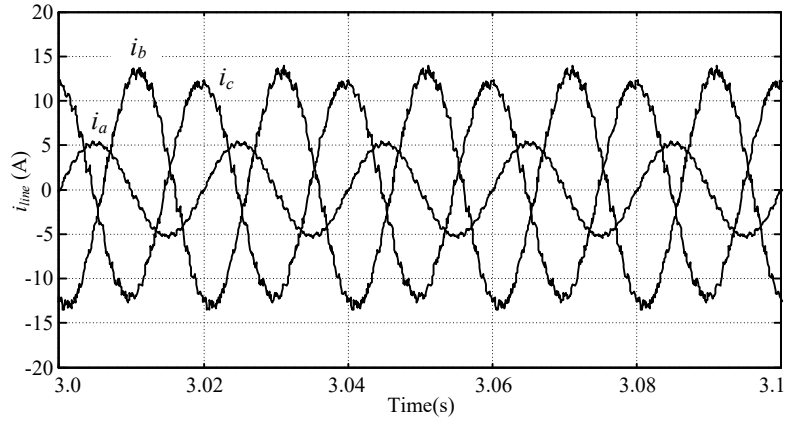


Figure 8: currents of three-phase system {Case-A}.

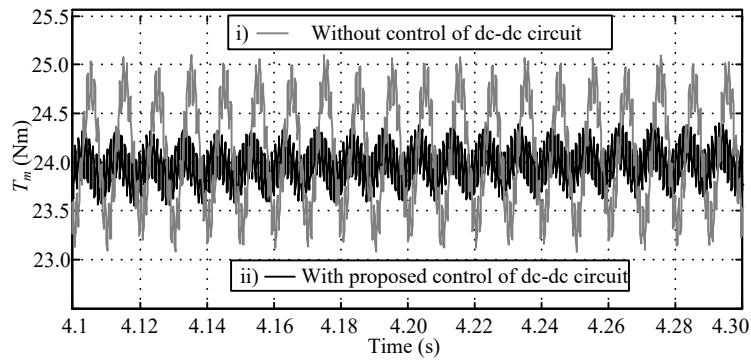


Figure 9: Torque response {Case-A}.

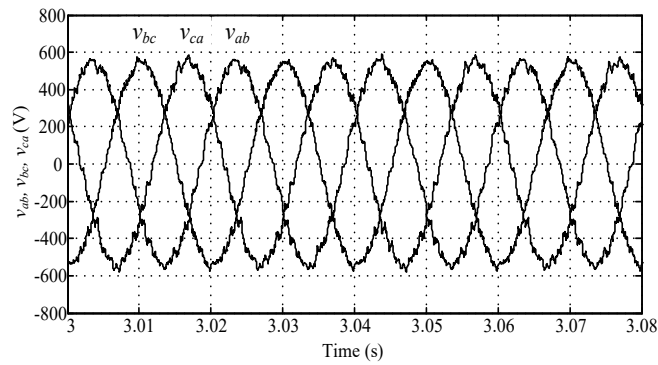


Figure 10: Voltages {Case-A}.

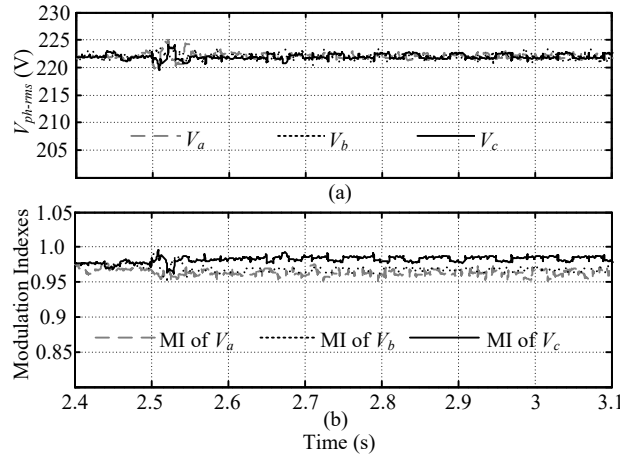


Figure 11: (a) Voltage; (b) MI{Case-A}.

### Case-B: Operation under battery and electrolyzer

The system's performance is dependent on the operational characteristics of the electrolyzer. This is achieved by regulating the State of Charge (SoC) of the batteries to approximately 80% and assuming the availability of excess power

from alternative sources. According to the energy management system described in this document, the electrolyzer starts using surplus power when the State of Charge (SoC) of the battery bank goes above 80.0%, as shown in Figure 12. According to the data depicted in Figure 13, it is evident that the State of Charge (SoC) attains a value of 80.0% at approximately  $t=1.95$  seconds. The voltage characteristics of the direct current (DC) bus, which is currently being regulated by the buck converter of the electrolyzer, are illustrated in Figure 13.

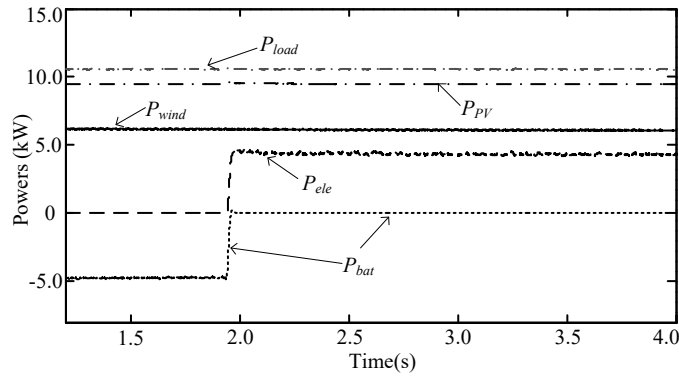


Figure 12: Powers involved in microgrid during operation of electrolyzer {Case-B}.

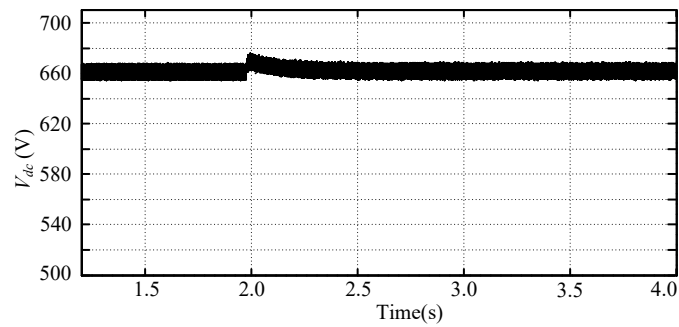


Figure 13: Voltage {Case-B}.

**Case-C: Operation with battery and FC**

The microgrid's performance during fuel cell (FC) operation was evaluated by analyzing the impact of a sudden load increase from 7.5 to 15.0 kW at  $t=10.0$  sec. As per the proposed energy management system, the battery exhibited a rapid response to fulfill the increased load requirement, whereas the fuel cell gradually initiated power supply owing to its slower dynamics. Consequently, the State of Charge (SoC) of the battery bank decreased to 20.0% at around  $t=10.94$  seconds (Figure 14). The frequency converter (FC) initiated power delivery at time  $t=11.16$  seconds and successfully fulfilled the load demand by approximately  $t=12.80$  seconds. The successful coordination between the fuel cell (FC) and battery resulted in the progressive reduction of battery capacity, as the FC consistently supplied the required electrical energy. The control scheme of the microgrid effectively achieved coordination, as illustrated in Figure 15.

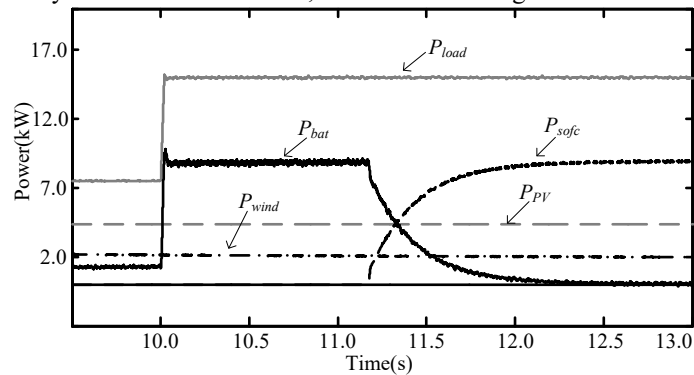


Figure 14: Powers {Case-C}.

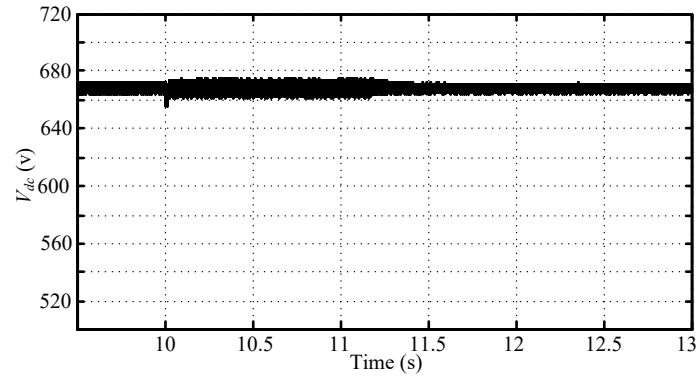


Figure 15: Voltage {Case-C}

**Case-D: Operation with meteorological changes**

The assessment of the microgrid's effectiveness incorporates considerations of meteorological variations in atmospheric conditions. The evaluation encompasses the quantification of irradiance, velocity, load, and temperature parameters, as illustrated in Figure 16. Figure 17 depicts the different power components examined in this study, including the battery bank, FC (Fuel Cell), and electrolyzers. The aforementioned components work together to establish a balanced state of power generation and load. The precise details pertaining to the root mean square (RMS) line voltage at the point of common coupling (PCC) can be located in Figure 18. Although the RMS voltage at the point of common coupling (PCC) may not offer a conclusive indication, the instantaneous line-to-line voltages and currents are depicted in Figure 19 and Figure 20, respectively.

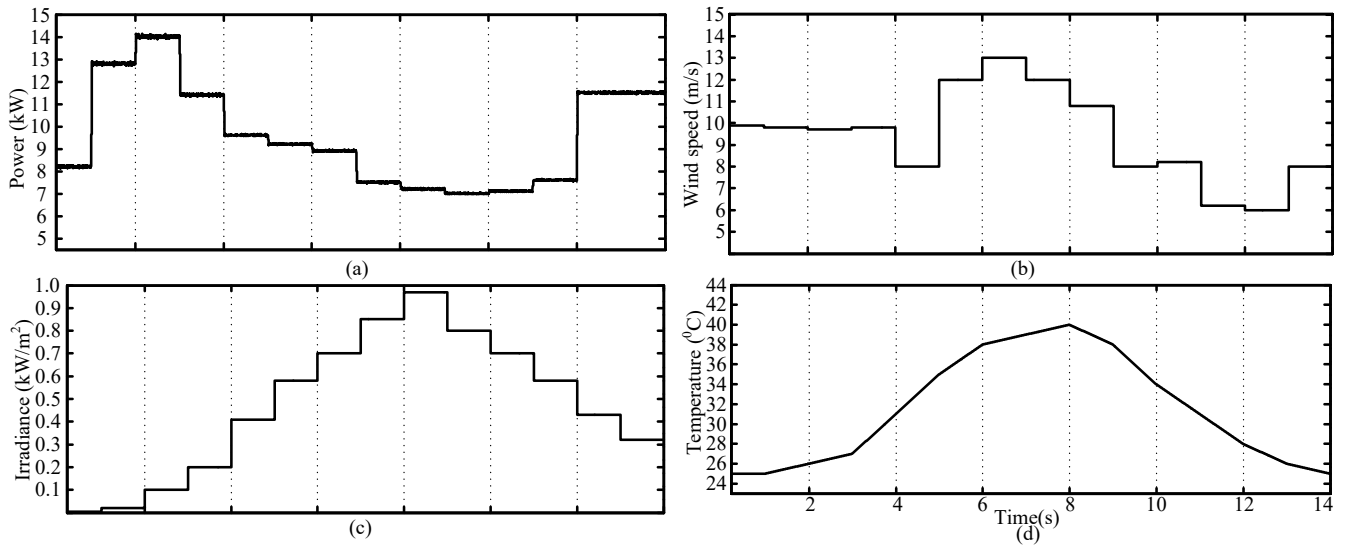


Figure 16: Changes of (a) load current, (b) wind speed, (c) irradiance and (d) temperature {Case-D}.

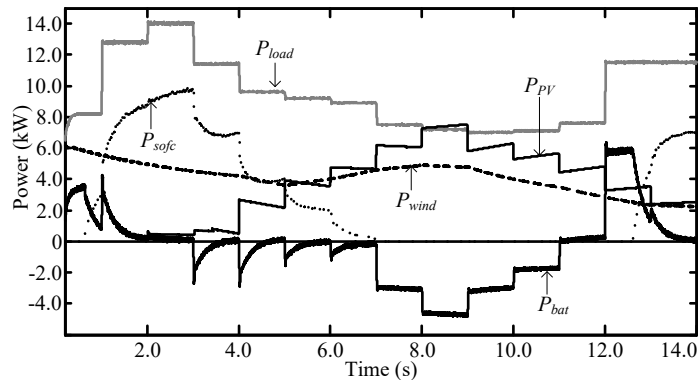


Figure 17: powers involved in microgrid {Case-D}.



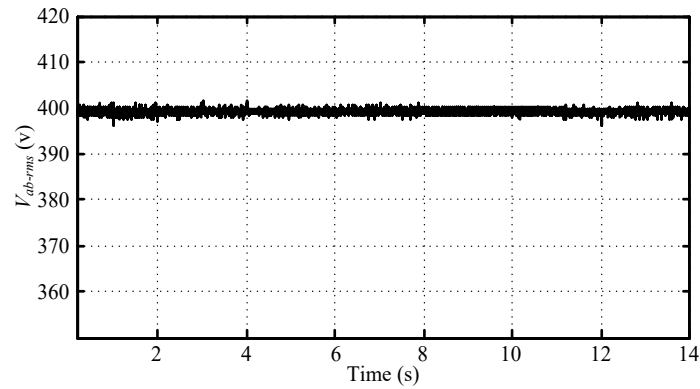


Figure 18: Voltages {Case-D}.

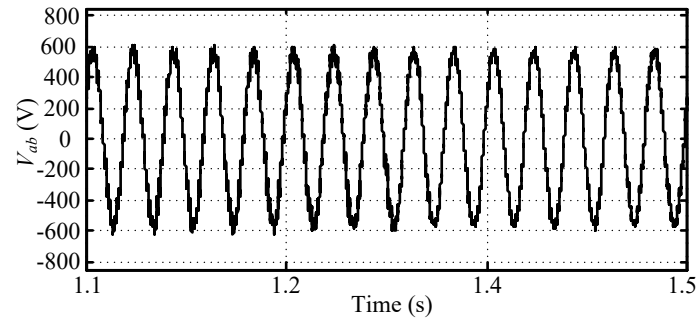


Figure 19: Voltages {Case-D}.

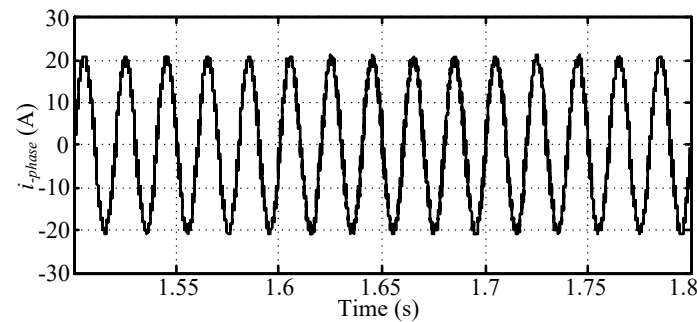


Figure 20: Currents {Case-D}.

## V. Conclusion

An energy management system with high optimization capabilities has been effectively implemented for microgrids that rely on renewable energy sources. The system utilizes synchronized control techniques to improve power quality and optimize hydrogen generation efficiency, leading to decreased operational costs. The suggested control techniques are specifically developed to address second harmonic distortions caused by imbalanced loads and guarantee voltage stability at the point of common coupling (PCC). Through the utilization of Simulink simulations, empirical evidence has demonstrated that the proposed controllers possess the capability to effectively regulate load voltages, even in the presence of varying loads, wind speeds, and solar radiation levels. The results have been subjected to analysis and have been presented in various scenarios for the purpose of evaluation.

## References:

- [1]. C. N. Bhende, S. Mishra and S. G. Malla, "Permanent Magnet Synchronous Generator-Based Standalone Wind Energy Supply System," *IEEE Transactions on Sustainable Energy*, vol. 2, no. 4, pp. 361-373, Oct. 2011, doi: 10.1109/TSTE.2011.2159253.
- [2]. H. U. R. Habib et al., "Optimal Planning and EMS Design of PV Based Standalone Rural Microgrids," in *IEEE Access*, vol. 9, pp. 32908-32930, 2021, doi: 10.1109/ACCESS.2021.3060031.
- [3]. M. H. Saeed, W. Fangzong, B. A. Kalwar and S. Iqbal, "A Review on Microgrids' Challenges & Perspectives," in *IEEE Access*, vol. 9, pp. 166502-166517, 2021, doi: 10.1109/ACCESS.2021.3135083.
- [4]. D. Steward, G. Saur, M. Penev and T. Ramsden, "Lifecycle Cost Analysis of Hydrogen Versus Other Technologies for Electrical Energy Storage", *Technical Report, National Renewable Energy Laboratory (NREL)*, Nov. 2009.
- [5]. W. Jiang and B. Fahimi, "Active Current Sharing and Source Management in Fuel Cell-Battery Hybrid Power System", *IEEE Transactions on Industrial Electronics*, Vol. 57, No. 2, pp. 752-761, Feb. 2010.
- [6]. Kandi Bhanu Prakash, "Modeling of DC to DC Converter for Renewable Energy Sources", *International Journal of New Technologies in Science and Engineering (IJNTSE)*, Vol. 9, Issue. 1, pp. 6-10, Jan. 2023.

- [7]. C. Wang and M. H. Nehrir, "Power Management of a Stand-Alone Wind/Photovoltaic/Fuel Cell Energy System", *IEEE Transactions on Energy Conversion*, Vol. 23, No. 3, pp. 957-967, Sep. 2008.
- [8]. Kodjo Agbossou, Mohanlal Kolhe, Jean Hamelin and Tapan K. Bose, "Performance of a Stand-Alone Renewable Energy System Based on Energy Storage as Hydrogen", *IEEE Transactions on Energy Conversion*, Vol. 19, No. 3, pp. 633-640, Sept. 2004.
- [9]. H. Caliskan, I. Dincer and A. Hepbasli, "Energy, Exergy and Sustainability Analyses of Hybrid Renewable Energy Based Hydrogen and Electricity Production and Storage Systems: Modeling and Case Study", *Applied Thermal Engineering*, In press (available online 21 April 2012).
- [10]. W. Gao, V. Zheglov, G. Wang and S. M. Mahajan, "PV - Wind - Fuel Cell - Electrolyzer Micro-grid Modeling and Control in Real Time Digital Simulator", *International Conference on Clean Electrical Power*, USA, pp. 29-34, June 2009.
- [11]. D. Ipsakis, S. Voutetakis, P. Seferlis, F. Stergiopoulos and C. Elmasides, "Power Management Strategies for a Stand-Alone Power System using Renewable Energy Sources and Hydrogen Storage", *International Journal of Hydrogen Energy*, Vol. 34, No. 16, pp. 7081-7095, Aug. 2009.
- [12]. O. Erdinc and M. Uzunoglu, "The Importance of Detailed Data Utilization on the Performance Evaluation of a Grid-Independent Hybrid Renewable Energy System", *International Journal of Hydrogen Energy*, Vol. 36, No. 20, pp. 12664-12677, Oct. 2011.
- [13]. E. Dursun and O. Kilic, "Comparative Evaluation of Different Power Management Strategies of a Stand-Alone PV/Wind/PEMFC Hybrid Power System", *International Journal of Electrical Power and Energy Systems*, Vol. 34, No. 1, pp. 81-89, Jan. 2012.
- [14]. P. Enjeti and S. Kim, "A new DC-side active filter for inverter power supplies compensates for unbalanced and nonlinear loads," *Proceedings of IEEE Industry Applications Society Annual Meeting*, Vol. 1, pp. 1023-1031, 1991.
- [15]. Z. W. Geem, "Size Optimization for a Hybrid Photovoltaic-Wind Energy System", *International Journal of Electrical Power and Energy Systems*, Vol. 42, No. 1, pp. 448-451, Nov. 2012.
- [16]. Phommixay, Sengthavy, et al. "Review on the cost optimization of microgrids via particle swarm optimization", *International Journal of Energy and Environmental Engineering*, vol. 11, no. 1, Mar. 2020.
- [17]. R. Robichaud, G. Mosey and D. Olis, "Renewable Energy Optimization Report for Naval Station Newport", *Technical Report NREL*, Feb. 2012.